DOI: 10.1038/ncb2796

nature cell biology

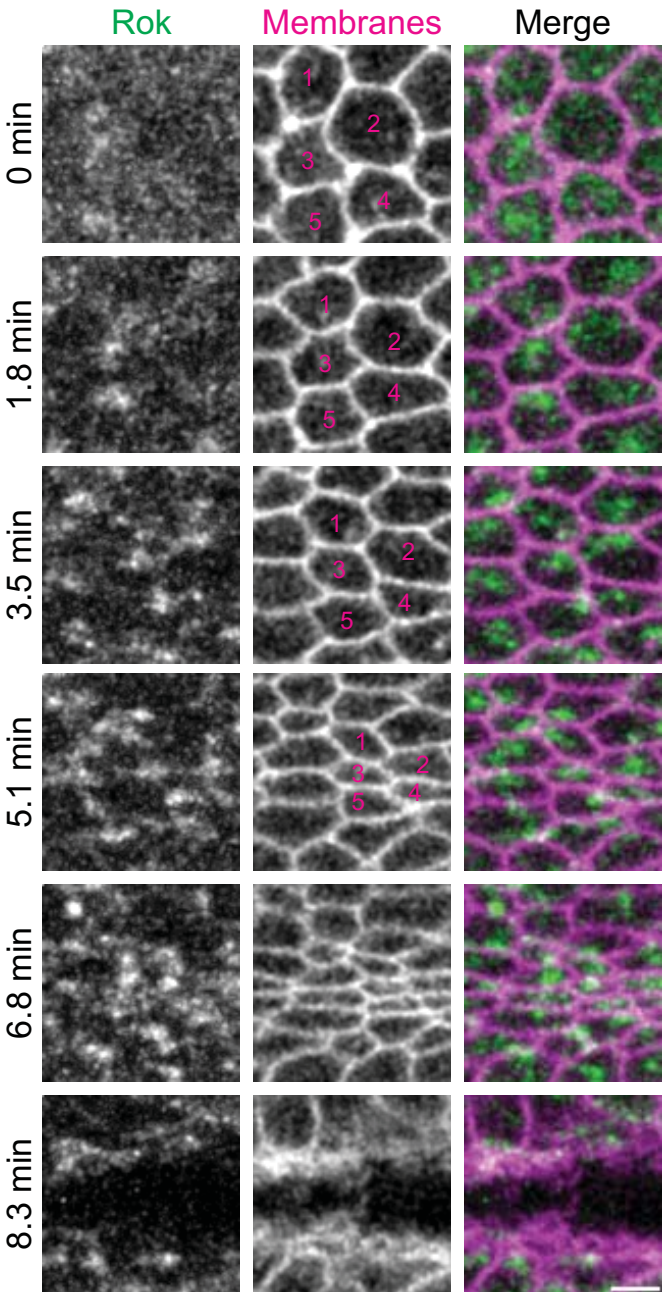

Figure S1 Venus::Rok(K116A) localizes to medioapical foci during constriction. During apical constriction, Venus::Rok(K116A) accumulates in medioapical foci in ventral furrow cells, similar to Venus::Rok(WT). Images are from a live embryo expressing Gap43::ChFP (subapical slice) and Venus::Rok(K116A) (apical projection). Apical constriction appears to be unaffected by expression of Rok(K116A). Scale bar is 5μm.

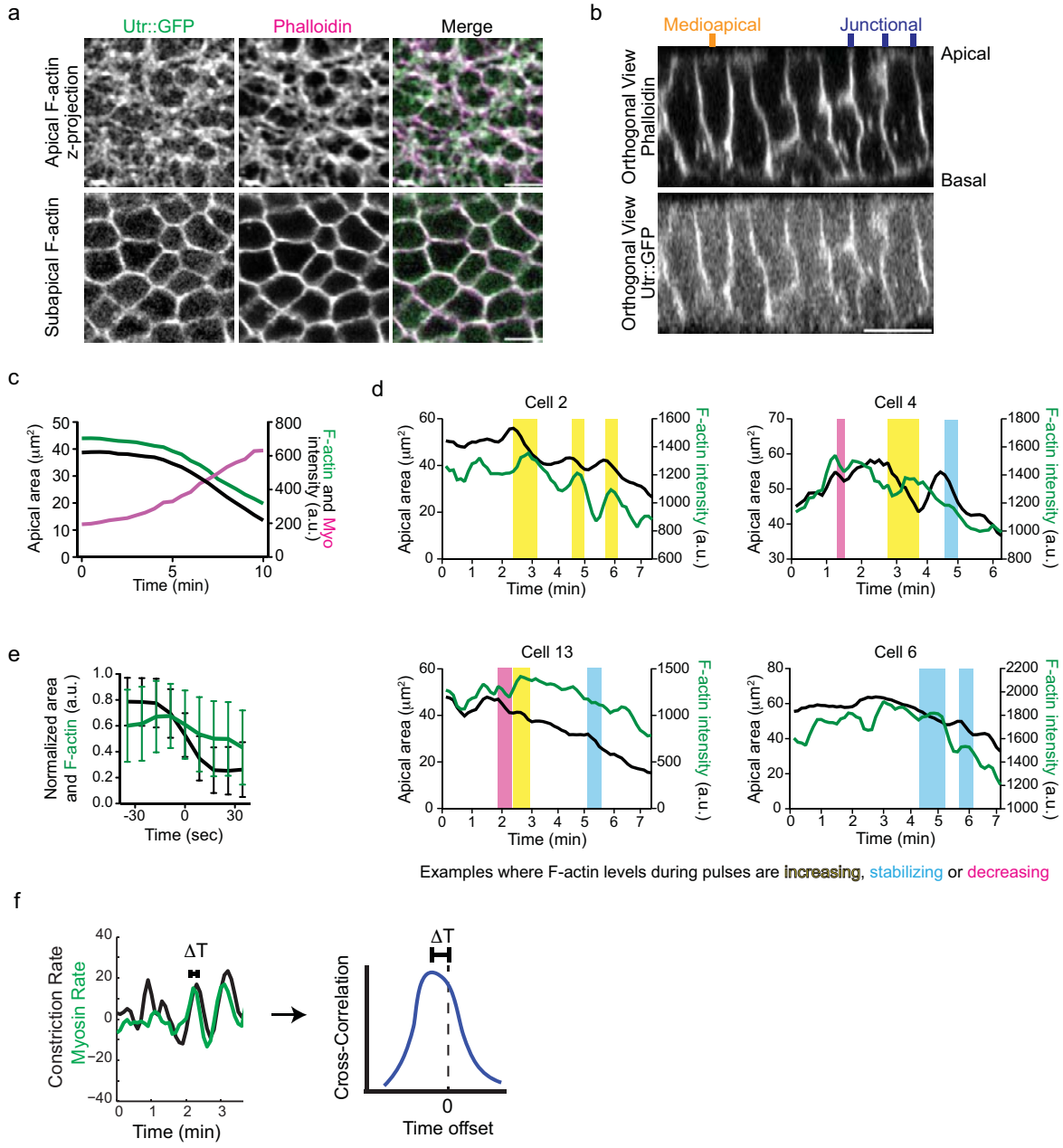

Figure S2 Apical F-actin is dynamic in ventral furrow cells. **(a)** Utrophin::GFP (Utr::GFP) labels F-actin throughout the cell, including medioapical, junctional, and subapical structures. Images are from fixed Utr::GFP embryo and stained with phalloidin to label F-actin. Scale bar is 5μm. **(b)** Orthogonal view/cross-section of same embryo from **a**. Scale bar is 10μm. **(c)** Total F-actin levels decrease throughout apical constriction. Quantifications are averages from embryos (n=4 embryos, at least 35 cells per embryo) expressing Utr::GFP and Myo::ChFP. Area was quantified from sub-apical F-actin images. Total apical F-actin and Myo-II levels were quantified from apical z-projections. Values for individual cells were averaged within an embryo and then averaged across multiple embryos. **(d)** Quantification of total F-actin levels and area in individual cells from a live embryo expressing Utr::GFP and Gap43::ChFP. F-actin levels during contractile pulses (highlights) are heterogeneous, and can increase (yellow), stabilize (blue), or decrease (magenta). F-actin levels most often increase or remain stable during a contractile pulse. **(e)** Graph of average behavior of area and F-actin during contractile pulses (n=44 pulses) from embryo in **d**. Values are normalized to highest and lowest values during individual pulses. Error bars are standard deviation. On average, F-actin levels are briefly stabilized during contractile pulses. **(f)** Schematic illustrating the calculation of the time resolved cross-correlation function. Cross-correlation is calculated between constriction rate and myosin rate for various temporal shifts (ΔT). A peak cross-correlation at ΔT~0 indicates a significant correlation with the value of ΔT indicating the time lag between the two signals.

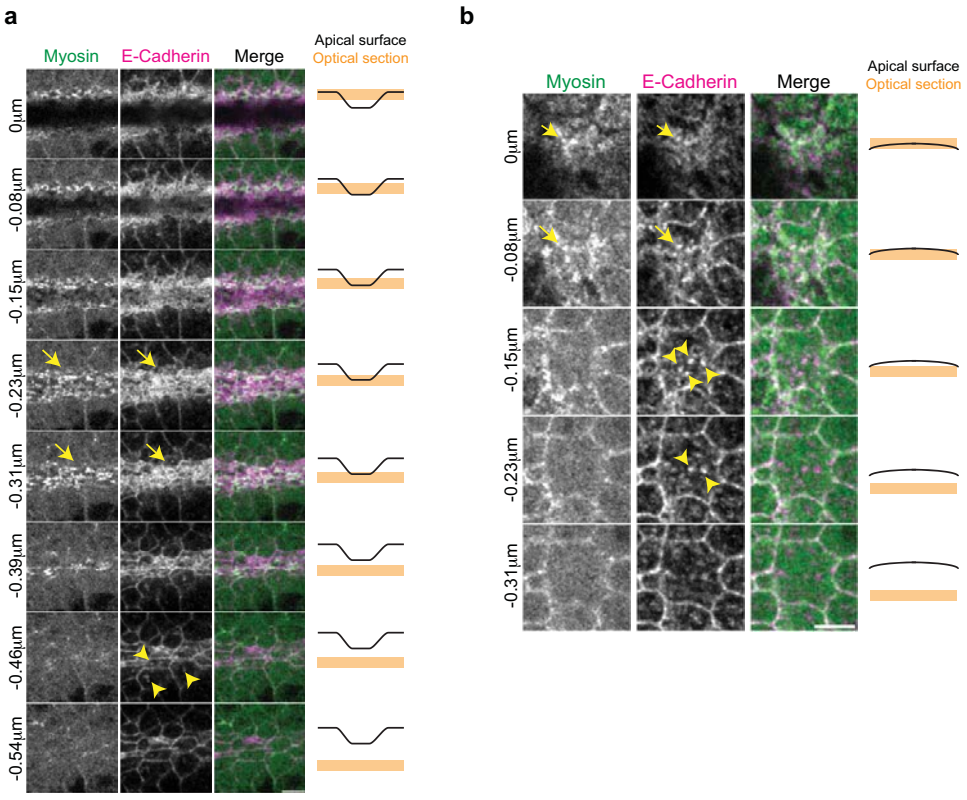

Figure S3 E-Cadherin localizes across the medioapical surface in *dia*^{M} mutants. a,b) Serial z-sections of confocal images from two different fixed *dia*^{M} embryos expressing Myo::GFP and stained for E-Cadherin. Medioapical E-Cadherin appears to be associated with the cortex and is localized in the same plane as Myo-II (arrows). Medioapical E-Cadherin in *dia*^{M} mutants can be distinguished from subapical E-Cadherin puncta that are likely to represent endocytic vesicles. Distances indicated are positions relative to the apical z-slice (0µm). Scale bars are 5µm.

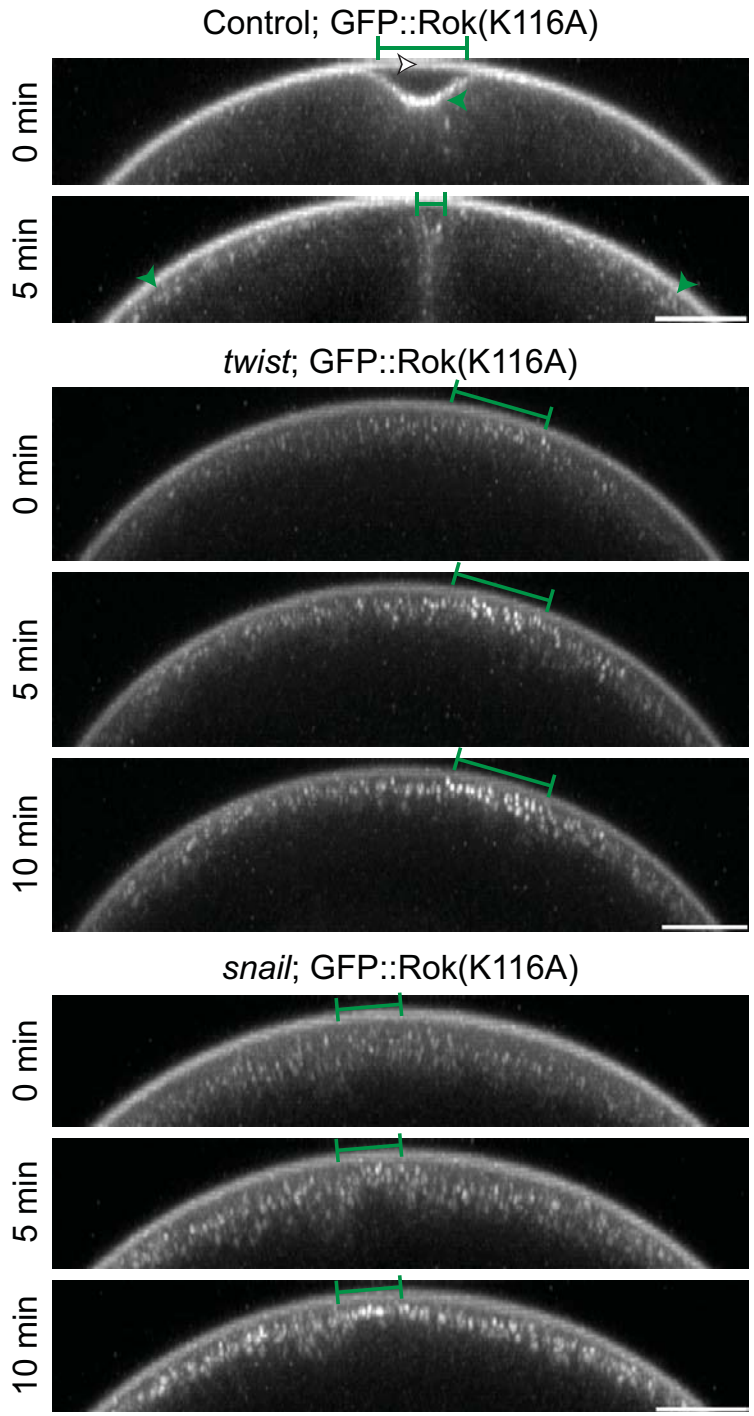

Figure S4 Snail is required for dorsal-ventral polarity of apical Rok localization. Control (*twist*/+) and *twist* mutants have apical GFP::Rok(K116A) (green arrowhead) enrichment in the ventral furrow (green bracket) prior to accumulation in germband cells (green arrowheads). White arrowhead marks the vitelline membrane. *snail* mutants accumulate GFP::Rok(K116A) in the ventral furrow and in germband cells at the same time. Images are projections of cross-sections from live control, *twist*, or *snail* embryos expressing GFP::Rok(K116A). Scale bars are 20μm.

Supplemental Video Legends

Supplemental Video 1: F-actin and Myo-II structures colocalize as apical Myo-II accumulates. Live imaging of embryo expressing the F-actin marker Utr::GFP (left, green) and Myo::ChFP (middle, magenta). Images are apical surface projections and were acquired at 6.16s intervals. The video is displayed at 10 frames per second (fps). Scale bar is 5μm, which is about the diameter of a cell.

Supplemental Video 2: F-actin cables form a dynamic medioapical meshwork in ventral furrow cells. Live imaging of control buffer (water) injected Utr::GFP embryo. Images are single z-slice and were acquired at 0.78s intervals. The video is displayed at 30 fps. Scale bar is 5μm.

Supplemental Video 3: Rok inhibition prevents medioapical F-actin condensation, but not F-actin cable assembly. Apical projection of F-actin (Utr::GFP) in Rok inhibitor, Y-27632, injected embryo (several cells shown). F-actin cables exhibit assembly and disassembly across the apical surface, both medioapically and at junctions. F-actin cables fail to condense after Rok inhibition. Images were acquired at 4s intervals. The video is displayed at 15 fps. Scale bar is 5μm.

Supplemental Video 4: Myo-II assembly and ventral furrow formation in control embryo. Apical projection of Myo-II::GFP (green) shows accumulation over time, and Myo-II induces pulsatile contraction of cell membranes (Gap43::ChFP, magenta, single subapical z-slice) in solvent (control) injected embryo. Image was acquired at 5.6s intervals. The video is displayed at 20 fps. Scale bar is 20μm.

Supplemental Video 5: CyoD disrupts Myo-II medioapical network connectivity. While Myo-II (green, apical projection) can accumulate and cells constrict, injection of CytoD (0.125mg/mL) disrupts the attachment of medioapical Myo-II to the junctional domain and a failure of cells to maintain cell-cell connectivity. Medioapical Myo-II networks can be seen repeatedly losing and regaining connections. Images are from CytoD injected Myo::GFP, Gap43::ChFP embryo (magenta, single subapical z-slice). Images were acquired at 5.6s intervals and every fourth frame is shown. The video is displayed at 7 fps. Scale bar is 20μm.

Supplemental Video 6: CytoD destabilizes the connection between the medioapical Myo-II network and junctions.
Medioapical Myo-II (green, apical projection) networks lose and regain connections when F-actin assembly is decreased by CytoD (0.125mg/mL). Magnified view of embryo expressing Myo::GFP and Gap43::ChFP (magenta, single z-slice) from Video 4. Image acquired at 5.6s intervals. The video is displayed at 20 fps. Scale bar is 5μm.

Supplemental Video 7: CytoD injection results in gaps in the apical F-actin meshwork. CytoD injection causes gaps in the F-actin meshwork followed by medioapical and juctional F-actin networks repeatedly losing and regaining connections, similar to Myo-II. CytoD (0.25mg/mL) was injected into Utr::GFP embryo and images are apical projection of F-actin (green) and subapical projection marking cell boundaries (magenta). Images were acquired at 7.2s intervals. The video is displayed at 15 fps. Scale bar is 5μm.

Supplemental Video 8: *dia*^{M} phenotype resembles CytoD injection. Myo-II (apical projection) forms dense meshwork across ventral furrow cells in control (*dia*/+) embryos (top embryo). In *dia*^{M} embryos (bottom embryo) Myo-II (apical projection) accumulates, but networks lose and regain connectivity (left side of embryo), similar to embryos injected with CytoD. Both control and *dia*^{M} embryos express Myo::GFP. Control embryo images were acquired at 8.8s intervals. *dia*^{M} embryo images were acquired at 9.3s intervals. The video is displayed at 20 fps. Scale bars are 20μm.

Supplemental Video 9: Snail and Twist are required for a medioapical meshwork of F-actin cables. Control (*twist*/+, left), *snail* (center), and *twist* (right) embryos expressing Utr::GFP demonstrate that both Snail and Twist are required for medioapical F-actin cable assembly during ratchet-like constriction. Control embryos have dense medioapical F-actin network that is dynamic as cells constrict and tissue invaginates. *snail* mutants have F-actin puncta that fail to form proper meshwork of F-actin cables. *twist* mutants have junctional F-actin cables and condense medioapical F-actin structures, but F-actin cables fail to form/persist. Images were acquired at 9.3s intervals for control, 7.4s intervals for *snail*, and 6s intervals for *twist*. The video is displayed at 15 fps. Scale bars are 5μm.